

The PAH 7.7 μm /850 μm ratio as new diagnostics for high extinction in ULIRGs – increasing evidence for a hidden quasar in Arp 220*

M. Haas¹, U. Klaas¹, S. A. H. Müller², R. Chini², and I. Coulson³

¹ Max-Planck-Institut für Astronomie (MPIA), Königstuhl 17, 69117 Heidelberg, Germany

² Astronomisches Institut, Ruhr-Universität Bochum, 44780 Bochum, Germany

³ Joint Astronomy Centre, 660 N. Aohuku Place, University Park, Hilo 96720, Hawaii, USA

Received 11 December 2000 / Accepted 11 January 2001

Abstract. A new method is presented to reveal high mid-infrared (MIR) extinction in ultraluminous infrared galaxies (ULIRGs): the ratio between the PAH 7.7 μm feature and the sub-mm continuum at 850 μm . While the sub-mm radiation is optically thin and serves for normalization, any high MIR extinction reduces the observed PAH 7.7 μm strength. Since the emitters (PAH carriers) and the absorbers (large dust grains reemitting at 850 μm) are typically mixed along the line of sight, the new method probes the absorption along the entire dust column, and not only the properties of a shallow surface. 13 out of a sample of 15 ULIRGs as well as 20 normal galaxies of a comparison sample populate the same well confined range of the PAH 7.7 μm /850 μm flux ratio (4 ± 2). Their MIR extinction may be moderate. In contrast, two ULIRGs show an exceptionally low PAH 7.7 μm /850 μm ratio indicative of high extinction: UGC 5101 has $A_V(\text{mixed}) \approx 50$ consistent with former spectroscopic estimates. Arp 220 has a huge extinction of at least $A_V(\text{mixed}) \approx 110$, exceeding former estimates of $A_V(\text{screen}) > 45$ based on the [SIII] 18.7 μm /33.5 μm ratio. As an application of the new diagnostics, after dereddening of the central MIR continuum and with the assumption of a disk-like dust distribution seen under a tilted angle, we find increasing evidence for a hidden quasar in Arp 220.

Key words. ISM: dust extinction – galaxies: Arp 220 – ISM – quasars – starburst – infrared: galaxies

1. Introduction

AGN (active galactic nuclei) have been detected so far only in about a third of the nearby ULIRGs (Genzel et al. 1998), in the remaining two thirds they may have escaped detection due to enormous extinction (Sanders 1999). Since most of the known AGN are pronounced MIR emitters, the extinction required to hide an AGN must be very high, but so far no technique is known to probe the entire MIR extinction.

When the amount of extinction is determined exclusively from data, which are themselves affected by extinc-

tion – like the 9.7 and 18 μm silicate absorption features or the [SIII] 18.7 μm /33.5 μm line ratio –, the result can be biased toward too low values, representing only the properties of a shallow surface, but not the entire dust column. Yet, a robust technique is required which provides the order of extinction and clues to whether the absorbing dust is located in a foreground screen or whether it is mixed with the emitters.

Extinction estimates of ULIRGs have also been derived from longer wavelengths, for example the shape of the spectral energy distribution from the moderately affected far-infrared (FIR) to the optically thin sub-mm regimes. These spectra can be fitted by one modified blackbody with a single temperature. This approach, however, ignores the multitude of dust temperatures suggested from the patchy optical morphology, and the formally derived extinction values up to $A_V \approx 1000$ are questionable. Refinements using several modified blackbodies rely on the choice of the dust emissivity β and the decomposition into the various temperature components (Klaas et al. 1997; Lisenfeld et al. 2000; Klaas et al. 2001), hence the opacities cannot unambiguously be determined.

Send offprint requests to: M. Haas,
e-mail: haas@mpia-hd.mpg.de

* Based on observations with the James Clerk Maxwell Telescope JCMT, the Swedish ESO Submillimetre Telescope SEST and the Infrared Space Observatory ISO, an ESA project funded by Member States (especially France, Germany, The Netherlands and the UK) and with the participation of ISAS and NASA. The development and operation of ISOPHOT and the Postoperation Phase are supported by MPIA and funds from Deutsches Zentrum für Luft- und Raumfahrt.

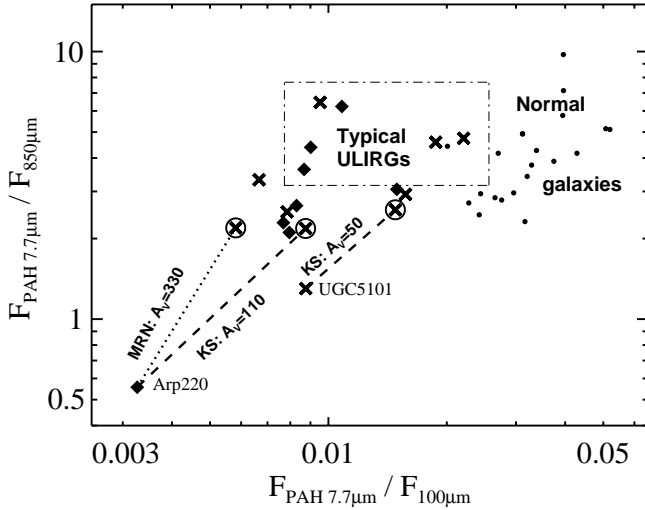


Fig. 1. Two-colour diagram PAH 7.7 μm to 850 μm flux versus PAH 7.7 μm to 100 μm . The symbols are: \times = Seyfert-ULIRGs, \blacklozenge = LINER- and HII/SB-ULIRGs, \bullet = normal galaxies. The errors are less than 30%. The positions of Arp 220 and UGC 5101 after dereddening are marked with the encircled crosses. For Arp 220 two mixed case extinction curves are considered: interstellar dust (MRN: dotted line), and protostellar dust (KS: dashed line). The dash-dotted box indicates the min-to-max range of the typical ULIRGs after dereddening with the KS model (Sect. 4.1) and A_V values from Genzel et al. (1998), note that dereddening reduces the PAH 7.7 μm /850 μm dispersion

2. The proposed new method and the database

In order to determine the total amount of extinction, we here propose a different method, using the PAH 7.7 μm to continuum 850 μm flux ratio. While the sub-mm radiation is optically thin and represents the emission from essentially all dust grains, the PAH strength (measured by the peak height of the Polycyclic Aromatic Hydrocarbons at 7.7 μm) is sensitive to dust extinction in the MIR. We apply this tool to 850 and 1300 μm observations of a sample of nearby bright ULIRGs (Klaas et al. 2001) most of which we recently obtained at the JCMT with SCUBA and at the SEST. These data, supplemented by literature data (Rigopoulou et al. 1996; Lisenfeld et al. 2000) and with the 1300 μm fluxes interpolated to 850 μm , are compared with published PAH spectra of ULIRGs, obtained with ISO (Rigopoulou et al. 1999) and with the UKIRT (Smith et al. 1989; Dudley 1999). This results in a sample of 15 ULIRGs with $L_{\text{FIR}} \approx 10^{12} L_{\odot}$ and both the sub-mm and PAH fluxes available.

A comparison sample of 20 “normal galaxies” was constructed as a subset of the SCUBA 850 μm local universe galaxy survey (Dunne et al. 2000) containing dusty galaxies with $L_{\text{FIR}} < 10^{10} L_{\odot}$. We selected those for which PAH spectra are available in the ISO data archive and for which the ISOPHOT-S aperture (24”) contains the entire 850 μm flux, as is the case for the ULIRGs.

The synchrotron contribution (clearly below 10%) has been subtracted from the 850 μm fluxes.

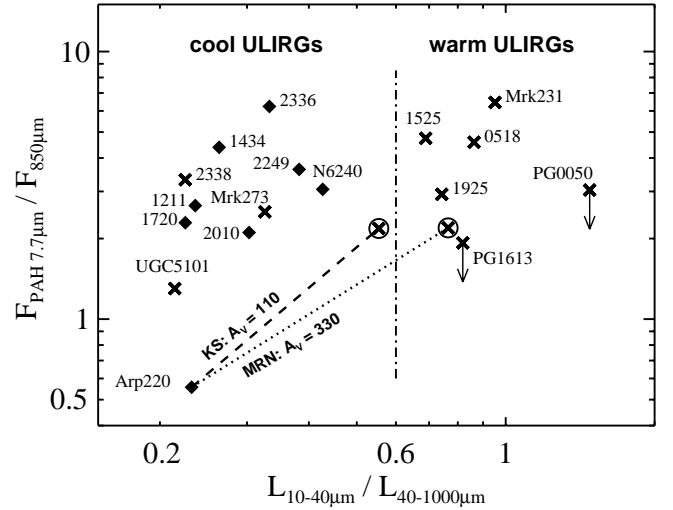


Fig. 2. Two-“colour” diagram PAH 7.7 μm to 850 μm flux versus $L_{\text{MIR}}/L_{\text{FIR}}$ ($= L_{10-40 \mu\text{m}}/L_{40-1000 \mu\text{m}}$). Symbols as in Fig. 1. In addition, two PG quasars, where PAH spectra are available, are plotted. The dereddened positions of Arp 220 correspond to the KS and MRN cases listed in Table 1. The vertical dash-dotted line marks the division between warm and cool ULIRGs according to $F_{25 \mu\text{m}}/F_{60 \mu\text{m}} \approx 0.2$

3. PAH 7.7 μm /850 μm measurements of high extinction

Figure 1 (y -axis) shows the PAH 7.7 μm /850 μm distribution of the ULIRGs and the reference sample.

Strikingly, all ULIRGs except Arp 220 and UGC 5101 lie in a confined range, which is also the same as for the normal galaxies. This suggests that for both samples the PAH and the sub-mm emission are related, and that no extraordinary excitation conditions are needed. The ISM in the galactic disk exhibits PAH emission with a low ISRF over a large range of different environmental parameters (Mattila et al. 1996). Léger & Puget (1989) predicted that PAH formation takes place in molecular clouds, and these are typically bright at 850 μm . UGC 5101 has a high mixed case extinction $A_V \approx 50$ derived from NIR-MIR spectroscopy (Genzel et al. 1998). Dereddening shifts it clearly into the range of the other ULIRGs (Fig. 1).

The PAH 7.7 μm /100 μm ratio is lower for the ULIRGs than for the reference sample by a factor of about three (x -axis in Fig. 1). ULIRGs have warmer dust ($30 \text{ K} < T < 50 \text{ K}$) than normal galaxies ($20 \text{ K} < T < 30 \text{ K}$), and therefore their 100 μm flux relative to that at 850 μm is higher. Again, along the PAH 7.7 μm /100 μm distribution Arp 220 lies below the other obviously more “typical ULIRGs” which populate a confined range. We consider three possibilities to explain the exceptional position of Arp 220 in Fig. 1:

1. A low PAH 7.7 μm flux due to destruction of the PAH carriers by a hard UV radiation field is unlikely, since this should be present in the other ULIRGs with exposed AGN like Mrk 231 and 0518. Yet there is no hint

Table 1. Observed and dereddened luminosities of Arp 220

	deredd. factor	L_{MIR} $10^{11} L_{\odot}$	deredd. factor	L_{FIR} $10^{11} L_{\odot}$	$L_{\text{MIR}}/$ L_{FIR}
observed	1.0	2.1	1.0	9.0	0.23
MRN: $A_V = 330$	10 (4...20)	≈ 21.0	3.2	28.8	0.72
KS: $A_V = 110$	4.0	8.4	1.7 (1.3 ... 2.0)	15.3	0.54
KS: $A_{V\text{screen}} = 90^*$	20.0	42.0	“	“	2.75

* Screen case on central MIR continuum, while the mixed case extinction probably still applies to the FIR emission.

for such a field in Arp 220. If present, it would already point towards a hidden AGN.

- An excess of 850 μm flux due to very cold dust which *also* has to be deficient in PAH emission: for example, the extremely quiet galaxy M 31 has very cold dust at $T \leq 16$ K (Haas et al. 1998) and it could be a low PAH emitter (Cesarsky et al. 1998). But in order to achieve the desired shift in Fig. 1, such very cold dust (even without any PAH emission) has to provide about half of the FIR emission and more than three quarters of the sub-mm emission of Arp 220. In this case the dust mass would approach (or even exceed) the molecular gas mass derived from the CO luminosities (Downes & Solomon 1998), resulting in a gas-to-dust ratio of about 5, unrealistically low compared with the standard value of about 150. Also, bearing in mind the ultraluminosity of Arp 220, a low excitation of the PAH carriers is unlikely.
- Extinction: since the first two mechanisms do not provide a satisfactory explanation, we conclude that the low PAH 7.7 $\mu\text{m}/850$ μm flux ratio of Arp 220 is mainly caused by extinction. Further evidence for a significant extinction comes from the deep silicate absorption feature (Dudley 1999). A comparison with UGC 5101 immediately suggests that the MIR extinction is very high.

To summarize, 13 out of 15 ULIRGs as well as 20 comparison galaxies populate the same confined range of the PAH 7.7 $\mu\text{m}/850$ μm flux ratio. Their MIR extinction may be moderate ($A_V \lesssim 3-10$), so that NIR-MIR spectroscopy can yield proper results. Also, it is not likely that they contain a hidden powerful AGN which has not yet been identified as such. Two ULIRGs, however, lie significantly below this range and their offsets are mainly due to high MIR extinction. The new PAH 7.7 $\mu\text{m}/850$ μm diagnostics is a promising tool to reveal high MIR extinction in ULIRGs.

4. Signatures favouring a hidden quasar in Arp 220

4.1. The amount of the PAH 7.7 μm extinction

Firstly, we argue in favour of the “mixed case” extinction, in contrast to the simpler case by a dust screen¹.

¹ The extinction factors are $\exp\{\tau_{\lambda}\}$ and $\tau_{\lambda}/(1-\exp\{-\tau_{\lambda}\})$ for the screen and the mixed case, respectively, with $\tau_{\lambda} = 0.916 \cdot A_{\lambda}$ (Genzel et al. 1998). For the same observed extinction

The difference in the PAH 7.7 $\mu\text{m}/100$ μm distributions between ULIRGs and the normal galaxies can be entirely explained by the higher 100 $\mu\text{m}/850$ μm colour temperature of the dust in ULIRGs. Hence, the PAH emitters do not appear particularly related to the warm – presumably starburst heated – dust in ULIRGs. Rather, the similar PAH 7.7 $\mu\text{m}/850$ μm distributions for the typical ULIRGs and the normal galaxies suggests that the PAH emitters and the sub-mm emitting dust grains are intimately coupled and actually mixed along the line of sight through the galaxies. Therefore, in the following we will use the mixed case, unless otherwise stated.

Now we consider the *minimum additional* mixed case extinction required to shift Arp 220 towards the lower border of the PAH 7.7 $\mu\text{m}/850$ μm range for the other ULIRGs (Fig. 1). This depends on the extinction curves used. $A_V \approx 330$, when using the interstellar extinction curve for graphite and silicate grains in our Galaxy, with a grain size distribution cutoff at about 0.3 μm (MRN-model: Mathis et al. 1983, Table C1).

In ULIRGs the dust may have properties more like those found in *protostellar* cold dense clouds. Their observed extinction curves have been successfully modelled using flaky grains with a large size cutoff at about 30 μm (KS model: Krügel & Siebenmorgen 1994). Using even larger grains (>30 μm) would result in a low emissivity exponent of $\beta < 1.2$, contrary to the observed value of $\beta \approx 1.6$ (Lisenfeld et al. 2000; Klaas et al. 2001). In contrast to the MRN model, the KS extinction curve has no 5–25 μm features in the MIR, consistent with the smooth curve observed toward the Galactic centre (Lutz et al. 1996). Therefore we give the KS model a slightly higher preference. If the *entire* dust in Arp 220 has such properties², then the extinction required to provide the PAH 7.7 $\mu\text{m}/850$ μm offset to the other ULIRGs is at least $A_V \approx 110$, which we adopt as a conservative estimate. It is also consistent with the lower limit $A_V(\text{mixed}) > 110$, which corresponds to $A_V(\text{screen}) > 45$ derived from [SIII] 18.7 $\mu\text{m}/33.5$ μm line ratio (Genzel et al. 1998). *Our value*

curves, the amount of extinguishing dust has to be much higher in the mixed case, since the emitters at the shallow surface are practically not extinguished and those deeply embedded have to be more heavily obscured. Thus, e.g. $A_V(\text{KS-screen}) \approx 60$ corresponds to $A_V(\text{KS-mixed}) \approx 250$. The length and orientation of the dereddening vectors in Fig. 1 remain practically unchanged, just the amount of extinction alters.

² We used: $A_V : A_{7.7 \mu\text{m}} : A_{15 \mu\text{m}} : A_{25 \mu\text{m}} : A_{60 \mu\text{m}} : A_{100 \mu\text{m}} : A_{850 \mu\text{m}} = 1:0.039:0.039:0.036:0.015:0.0076:0.00035$.

$A_V(\text{mixed}) \approx 110$ is a lower limit, since it refers to the minimum extinction required to shift Arp 220 to the range of the other ULIRGs.

4.2. The extinction of the MIR continuum

So far, we have derived the *average* extinction of Arp 220 which, however, could vary between *different lines of sight*.

The central region of Arp 220 exhibits a complex geometry on NICMOS images (Scoville et al. 1999) with two nuclei, each intersected by dust lanes, which are coincident with the CO disks (Downes & Solomon 1998). At $2 \mu\text{m}$ the actual nuclear centres appear to be entirely hidden behind the dust lanes. On KECK high resolution $3\text{--}24.5 \mu\text{m}$ images the PAH emission, the silicate absorption and the $12.5 \mu\text{m}$ continuum show similar morphologies and only a moderate variation in the intensity ratios for various image areas (Soifer et al. 1999). Most of the MIR emission arises from an extremely compact area with a diameter of less than 100 pc centred on the western nucleus (Soifer et al. 1999). It contributes to the total flux by 66% at the $12.5 \mu\text{m}$ continuum and 55% at the $7.7 \mu\text{m}$ PAH line.

We argue now, that the extinction of the western nuclear MIR continuum is higher than previously inferred. If the extinction of the western nucleus were actually as low ($A_V \approx 25$) as inferred from the $18 \mu\text{m}$ silicate absorption, then its dereddening does not increase the PAH strength significantly.

In this case the “rest” (= total – western nucleus) of Arp 220 must contain all the hidden PAH emission necessary to reach the PAH $7.7 \mu\text{m}/850 \mu\text{m}$ and PAH $7.7 \mu\text{m}/100 \mu\text{m}$ levels of the other ULIRGs. Hence this “rest” has to be much more extinguished ($A_V(\text{rest}) \approx 1.7 \cdot A_V(\text{average})$). But this contradicts to the moderate variation in the intensity ratios for various image areas emphasized above. Furthermore, a detailed calculation shows that the dereddened position of the entire galaxy Arp 220 then lies in the same range as for the simple average dereddening (Fig. 1). Since the silicate absorption feature may probe only the shallow surface, the actual extinction of the western nucleus may well be much higher than $A_V \approx 25$.

These arguments support the picture that in Arp 220 both the regions emitting the PAH $7.7 \mu\text{m}$ and those emitting the $12.5 \mu\text{m}$ continuum are affected by a high MIR extinction of similar order of $A_V(\text{mixed}) \gtrsim 110$. Thus the extinction is so high that it might be difficult to discover a hidden AGN with common tracers.

4.3. Dereddening of the MIR continuum

The effects of reddening depend on the geometry of the absorbing/remitting dust and we consider here the extreme cases “ideal sphere” and “axis-symmetric geometry”.

If the dust were distributed in an *ideal sphere*, then the absorbed MIR continuum could only escape via reemission at longer wavelengths. In this case “dereddening” will not

increase the total luminosity, but only the $L_{\text{MIR}}/L_{\text{FIR}}$ ratio via a shift of L_{FIR} towards L_{MIR} . But this case can be rejected as follows:

The presence of CO disks already indicates a *non-spherical axis-symmetric geometry* tilted about 45° with respect to our line of sight (Downes & Solomon 1998). Therefore, a significant portion of the MIR continuum might escape along the polar directions, but along the line of sight a reduced portion of the luminosity is seen. In order to derive the true MIR luminosity, dereddening has to be applied. It will actually increase L_{MIR} , and to a less extent L_{FIR} ³.

If the emitters of the MIR continuum are mixed with the absorbing dust, then the same A_V as derived from the PAH diagnostics can be used for dereddening. The results are listed in Table 1 and shown in Fig. 2.

Dereddening with the MRN model shifts Arp 220 from the cool ULIRGs to the warm ones, each of which houses a strong AGN. With the KS model such a shift is present, but less pronounced. Nevertheless, in both cases L_{MIR} reaches high quasar-like values ($\approx 10^{12} L_\odot$).

The compactness of the MIR emitting region and the presence of the dusty CO disks suggests, that the MIR continuum emitters are not as well mixed with the absorbing dust as the PAHs. This does not conflict with the low variation of the observed MIR colours across the KECK images mentioned above. In this case the (hidden) MIR continuum originates more in the centre, which is surrounded by the absorbing material. Such a situation is typically seen in Seyfert 2s (Clavel et al. 2000). Then half of the dust column according to $A_V(\text{KS mixed}) \approx 110$ will work effectively on the central MIR continuum as *screen* absorber with an amount of $A_V(\text{KS screen}) \approx 90$, placing Arp 220 clearly in the $L_{\text{MIR}}/L_{\text{FIR}}$ range of quasars (Table 1). With $A_V(\text{MRN mixed}) \approx 330$ the screen dereddening of the centre becomes even more extreme.

4.4. Compact starbursts versus powerful AGN

With conservative dereddening of L_{MIR} by a factor of 4 (Table 1, KS: $A_V \approx 110$), the MIR luminosity density of the *western nucleus* reaches $7.3 \cdot 10^7 L_\odot/\text{pc}^2$ ($L_{\text{MIR}} \approx 0.56 \cdot 10^{12} L_\odot$, $r \approx 50 \text{ pc}$), about a factor of 1000 higher than in the prototype nearby starburst galaxy M 82 ($L_{\text{MIR}} \approx 9 \cdot 10^9 L_\odot$, $r \approx 200 \text{ pc}$). Since the dust (and the gas) is more dissipative than the stars, it tends to be distributed in a more compact area than the stars. Bearing this in mind, it is difficult to imagine, how starbursts alone can create such a high luminosity density, and *simultaneously* how the dust hides them entirely.

³ Because the MRN extinction curve shows features between 5 and $25 \mu\text{m}$, we used luminosities. $L_{10-40 \mu\text{m}}$ comprises some kind of stable average over these features; our results are basically the same as when using e.g. the 12.8 or $15 \mu\text{m}$ fluxes. The luminosities of the sample are derived from ISOPHOT and sub-mm photometry (Klaas et al. 2001); we use $H_0 = 75 \text{ km s}^{-1}/\text{Mpc}$.

Therefore, a more natural explanation would be that – in addition to the prominent starbursts mainly responsible for the FIR luminosity – one (or perhaps both) of the nuclei of Arp 220 contains a powerful AGN providing the quasar-like MIR luminosity which is hidden to us.

To summarize, Arp 220 shows an extraordinarily high – presumably mixed case – extinction, which also works on the MIR continuum of the western nuclear region. The presence of tilted non-spherical geometry justifies that after dereddening the true MIR luminosity reaches quasar-like values. Moreover, the MIR luminosity density of the western nucleus exceeds that of known circumnuclear starbursts, thus increasing the evidence for a hidden quasar in Arp 220.

References

- Cesarsky, D., Lequeux, J., Pagani, L., et al. 1998, *A&A*, 337, L35
- Clavel, J., Schulz, B., Altieri, B., et al. 2000, *A&A*, 357, 839
- Downes, D., & Solomon, P. M. 1998, *ApJ*, 507, 615
- Dudley, C. C. 1999, *MNRAS*, 307, 553
- Dunne, L., Eales, St., Edmunds, M., et al. 2000, *MNRAS*, 315, 115
- Genzel, R., Lutz, D., Sturm, E., et al. 1998, *ApJ*, 498, 579
- Haas, M., Lemke, D., Stickel, M., et al. 1998, *A&A*, 338, L33
- Klaas, U., Haas, M., Heinrichsen, I., & Schulz, B. 1997, *A&A*, 325, L21
- Klaas, U., Haas, M., Müller, S. A. H., et al. 2001, *A&A*, submitted
- Krügel, E., & Siebenmorgen, R. 1994, *A&A*, 288, 929
- Léger, A., & Puget, J.-L. 1989, *ARA&A*, 27, 161
- Lisenfeld, U., Isaak, K. G., & Hills, R. 2000, *MNRAS*, 312, 433
- Lutz, D., Feuchtgruber, H., Genzel, R., et al. 1996, *A&A*, 315, L269
- Mathis, J. S., Mezger, P. G., & Panagia, N. 1983, *A&A*, 128, 212
- Mattila, K., Lemke, D., Haikala, L. K., et al. 1996, *A&A*, 315, L353
- Rigopoulou, D., Lawrence, A., & Rowan-Robinson, M. 1996, *MNRAS*, 278, 1049
- Rigopoulou, D., Spoon, H. W. W., Genzel, R., et al. 1999, *AJ*, 118, 2625
- Sanders, D. B. 1999, *Ap&SS*, 266, 331
- Scoville, N. Z., Evans, A. S., Dinshaw, N., et al. 1999, *ApJ*, 492, L107
- Smith, C. H., Aitken, D. K., & Roche, P. F. 1989, *MNRAS*, 241, 425
- Soifer, B. T., Neugebauer, G., Matthews, K., et al. 1999, *ApJ*, 513, 207